universe

MDPI

Article

Transient Flashes in Saturn's UV Aurora: An Analysis of Hubble Space Telescope 2013–2017 Campaigns and Cassini Magnetic Field Measurements

Tianshu Qin [1,*], Sarah V. Badman [1], Joe Kinrade [1] and Alexander Bader [2]

[1] Department of Physics, Lancaster University, Lancaster LA1 4YW, UK
[2] Gorilla, 2000 Antwerp, Belgium
* Correspondence: qintianshu2016@gmail.com

Abstract: We examined Hubble Space Telescope images of Saturn's northern UV aurora in 2013–2017, identified 29 short-lived flashes, and examined simultaneous magnetometer data collected by the Cassini orbiter. When observation cadence permitted, a flash lifetime of 4–17 min (subject to exposure time-related uncertainties), and a 40–70 min recurrence period were found. An occurrence map shows a strong preference in both local time (14–19 LT) and latitude (75–85°). These transient flashes are identified in both the presence and absence of Saturn's main auroral oval, indicating the lack of dependence on the main emission power. The concurrent magnetic field pulsations generally form a sawtooth shape, and the local field strength experiences a change of 0.2 to 2.0 nT (depending on the distance of Cassini). The quasiperiodic pulsation events were all detected when the spacecraft was in the southern hemisphere with conjugate flashes in northern aurora, suggesting these events occur on closed field lines, and typically showing a sudden transition to a less lagging, more southward magnetic field configuration. We also found the ionospheric footprint of the spacecraft must be close to the region of flashes for magnetic field pulsations to be detected, implying a localised rather than global driving process.

Keywords: aurora; pulsation; magnetosphere

Citation: Qin, T.; Badman, S.V.; Kinrade, J.; Bader, A. Transient Flashes in Saturn's UV Aurora: An Analysis of Hubble Space Telescope 2013–2017 Campaigns and Cassini Magnetic Field Measurements. *Universe* **2022**, *8*, 602. https://doi.org/10.3390/universe8110602

Academic Editors: Qiugang Zong, Zejun Hu, Zhonghua Yao and Jianjun Liu

Received: 28 September 2022
Accepted: 11 November 2022
Published: 17 November 2022

1. Introduction

Auroral flashes at Saturn were first observed in Hubble Space Telescope (HST) images by Radioti et al. [1], who indicated a possible association with energetic particle injections. Badman et al. [2] identified upward bursts of light ions (100–360 keV), energetic electrons (hundreds of keV) and broadband whistler waves during an interval of ∼1 h bifurcation signatures in the aurora. Radioti et al. [3] proposed a relation between quasiperiodic (QP) ∼1 h auroral bifurcations and magnetopause reconnection supported by the observation of cold dense electrons and "stepped" ion energy-latitude dispersions. Meredith et al. [4] examined small-scale transient features (10–30 min duration) with HST images for both northern and southern UV aurora and suggested they were produced on newly-opened field lines and were not conjugate between hemispheres. Mitchell et al. [5] reported another observation of repeated auroral intensifications at high latitudes and showed the accompanying ∼1 h pulsations in magnetic field, auroral hiss power and electron and ion energies, also suggesting recurrent reconnection events at the magnetopause as the driving mechanism. They also pointed out the rapid rotation (through 6 hours in LT from noon to dusk) of these auroral arcs as well as the involvement of the polar cap region.

Two statistical surveys [6,7] of the ∼1 h QP electron injection events (with hundreds of keV up to several MeV of energy) suggest a variable interpulse period (∼40–90 min) as well as a dawn-dusk asymmetry with ∼80% of the events identified in the duskside, indicative of a dominance by reconnection sites in the duskside. A survey of low-frequency waves (of periods 10–60 min) by Pan et al. [8] showed an intense population of magnetic fluctuations extending from the pre-noon sector to dusk, but a clear local minimum in the distribution was seen at ∼18 LT. Bader et al. [9] examined all available Cassini UVIS auroral sequences and also found an obvious location bias on the duskside for ∼1 h auroral flashes with duration < 20 min and emission power up to 50% of the total auroral power. They suggested a closed field configuration as the QP pulsation event was observed in both hemispheres, and a possible internal driving mechanism—a "drizzle" of small-scale magnetodisc reconnection events predominantly in the dusk flank, contributing to plasma circulation in this region.

The reconnection "drizzle" was proposed by Delamere et al. [10], who examined Cassini magnetometer (MAG) data for identified current sheet crossings in Saturn's magnetosphere and found large-scale reconnection events are insufficient to support the observations of large B_θ variations as well as frequent negative measurements in B_θ. They concluded that plasma can be lost through reconnection "drizzle" (a patchy network of small-scale reconnection sites), which are found predominately on the dusk flank. Studies of the dayside magnetodisc by Guo et al. [11,12] showed that magnetodisc reconnections can occur on the dayside, and, with potential corotation with the planet, the existence of internally driven "drizzle-like" dayside magnetodisc reconnection casts a reconsideration of the balance between internal and external drivers that control magnetic reconnection especially on the dayside.

In addition, the magnetospheric box model developed by Yates et al. [13] showed the ∼1 h QP magnetic field fluctuations are likely second harmonic Alfvén waves standing between the northern and southern ionospheres in the outer magnetosphere, and are modulated by the rocking of Saturn's magnetosphere. Yao et al. [14] proposed another possible link with wave characteristics—pulsating FACs generated by travelling Alfvén waves—when investigating a near-noon auroral feature of 30 min duration. Furthermore, Rusaitis et al. [15] suggested that solar wind periodic density structures could propagate into Saturn's magnetosphere and show up in the MAG data. They found these field perturbations spreading across both dayside and nightside local times with Alfvénic characteristics and proposed that the driving mechanisms were standing Alfvén waves driven from solar wind interaction at the magnetopause [15,16].

This research focuses on HST observations of Saturn's UV aurora during 2013–2017 in search for quasiperiodic auroral flashes and magnetic field measurements by Cassini's magnetometer in order to analyse the characteristics of conjugate field perturbations.

2. Data

2.1. Hubble Space Telescope Images

We use Hubble Space Telescope (HST) images of Saturn's northern UV aurorae from 2013–2017 taken by two instruments onboard, the Advanced Camera for Surveys (ACS) and the Space Telescope Imaging Spectrograph (STIS). The "F115LP" (passband 1150–2000 Å) and "F125LP" (1200–2000 Å) filters were used for the ACS (2013 images), and the "F25SrF2" (1250–1900 Å) filters were used for the STIS (2014–2017 images) while unfiltered images (1150–1900 Å) were also included in the 2014 campaign. Because of the use of different instruments and filters, the integration time of subexposures from different years varies—100 s for 2013 images, between 270 and 420 s for 2014 images, 450 s for 2016 images, and 500 s for 2017 images. These images have been previously presented by [17–19].

All images used in this study are processed using the pipeline developed at Boston University, including dark count subtraction, flat-fielding, correction for geometric distortion, and subtraction of an empirical background [20]. The photon counts are converted to units of kiloRayleigh (kR), which is a measure of photon flux, using the filter-specific conversion factors determined by Gustin et al. [21], and assuming a colour ratio (ratio of intensity in unabsorbed and absorbed wavebands) of 1.1. The images are projected onto a planetocentric polar grid with spatial resolution 0.25° × 0.25° (longitude × latitude) at an altitude of 1100 km above the 1-bar reference spheroid, which is equivalent to an on-planet resolution of ∼ 250 × 250 km.

2.2. Cassini Magnetometer

We use measurements of Saturn's magnetic field from the Cassini magnetometer [22]. We use 1-min sampled data, referenced using the Saturn-centred coordinate system-Kronocentric spherical coordinates (KRTP)—where the radial (r) component points radially from Saturn's centre to the spacecraft, the azimuthal (ϕ) component is parallel to kronographic equator and positive in the direction of corotation, and the southward (θ) component completes the right-hand set.

Cassini's orbital locations corresponding to the entire time sequence of HST images examined in this study are obtained using SPICE with the Kronocentric Solar Magnetic (KSMAG) coordinates and projected onto the HST polar plots. The magnetic footprint mapping from the spacecraft position was performed using the Dougherty et al. [23] model of the internal field, plus the Bunce et al. [24] model of the ring current for a standard magnetopause standoff distance of 21 Rs. This model does not include any azimuthal component of the field, i.e., no offset in LT between the spacecraft and its mapped ionospheric footprint. Comparison of different field models suggests an uncertainty of $\sim 2^{\circ}$ in the mapped latitude of the spacecraft [25]. The mapping of the spacecraft's real-time location enables us to link magnetic field measurements with the auroral events on a spatial scale (presented in the next section).

3. Results

3.1. Observations of Transient Auroral Flashes in HST UV Images

The observed characteristics introduced in Section 1 were used to guide the identifications of flashes in this study. Sequences of images were examined for evidence of bright flashes above the background emission. We assessed whether a transient was sufficiently coherent in shape and intensity (above noise levels) to be a flash, and if it appeared in consecutive images and HST orbits (when observing cadence permitted).

We examined HST observations from 36 days consisting of, in total, 548 images of Saturn's northern aurora in 2013-2017 and identified 29 transient flashing episodes (summarised in Table 1) over 21 different days. Three examples of typical transient auroral flashes are shown in Figure 1, and they are 2013-110 (Figure 1a–d), 2013-138 (Figure 1e–h) and 2013-139 (Figure 1i–l), where this date format denotes the day of year (DOY). The yellow arrows highlight the location of each identified flash, all in the duskside. These example flashes have a duration of 11 min (2013-110), 7 min (2013-138) and 8.7 min (2013-139), with uncertainties related to integration times. Images of 2013-110 and 2013-139 events show that the flashes in the duskside occurred while a main auroral arc of variable power was present either in the dawn-noon sector (Figure 1a–d) or on the nightside (Figure 1i–l), while images of the 2013-138 event (Figure 1e–h) show the flash occurred in the duskside with significantly fainter main oval emissions at other local times (LT). These three example flashes all take arc shapes extending for $\sim$3 h in LT and all sit in the duskside poleward of 15° colatitude. The flashes could evolve and potentially move in either azimuthal direction, but their movements are much less significant than further examples shown in Section 3.3, and the motion detection is limited by the imaging cadence. The red footprints in Figure 1 represent the simultaneous location of Cassini in Saturn's ionosphere. In these three examples, Cassini's location was mapped to the same region as the flashes although there is a $\geq$5° difference in latitude for the 2013-110 event (Figure 1a–d).

It is notable that no transient features matching the identifying criteria were observed in the dawnside in all 2013–2017 images, perhaps because in the conditions of high main auroral powers they could not be detected above these dynamics. However, they were also not detected in this region when the main emission was faint or absent (e.g., Figure 1e–h).

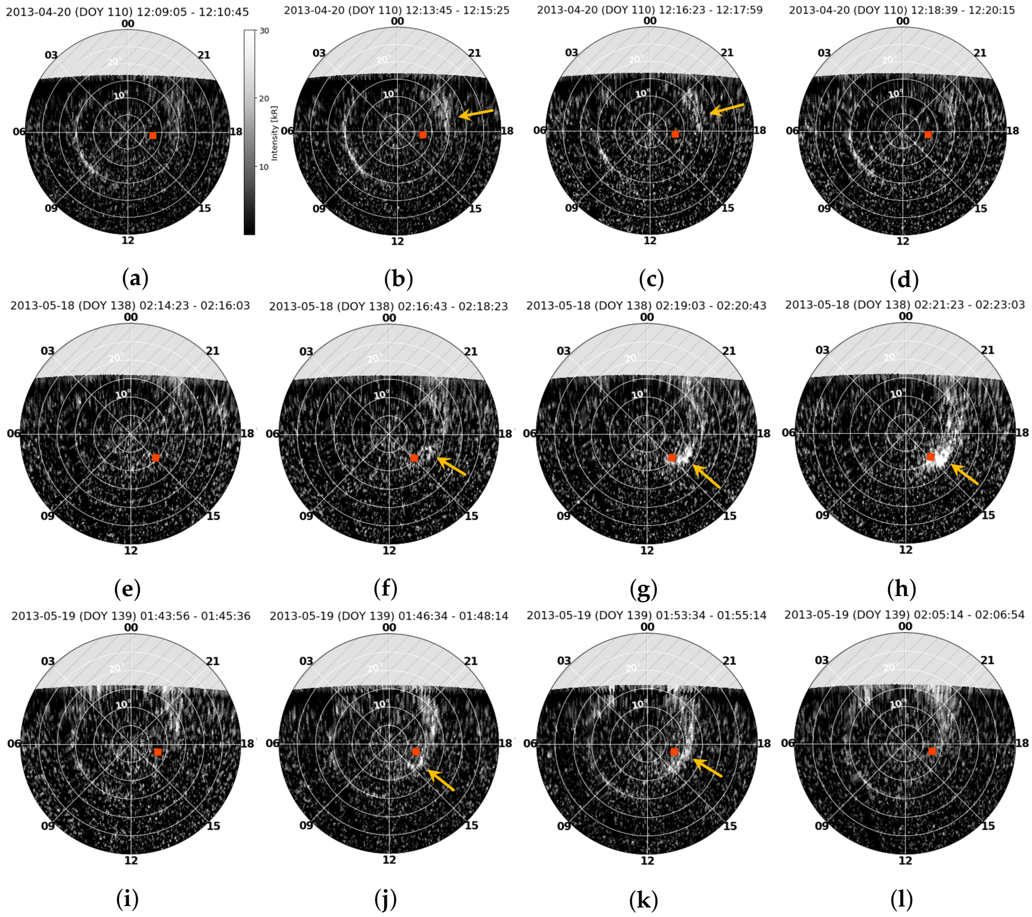

Figure 1. HST images of Saturn's northern hemisphere in polar projection covering the evolution of 2013-110 (event no. 1) (**a**–**d**), 2013-138 (event no. 5) (**e**–**h**) and 2013-139 (event no. 6) (**i**–**l**). 0–30° colatitude range was extracted hence the innermost ring in every plot stands for 5° colatitude (or 85° latitude) and each step in between is 5°. The longitude is represented in local hour starting from 0 at the top anti-clockwise, hence dawn is at 6 LT, noon at 12 LT and dusk at 18 LT. All panels share the same colour bar as (**a**) represnting the auroral intensity in kiloRayleigh (kR). The integration time of the 2013 images is 100 s. The yellow arrows highlight the identified transient flash, while the red footprints represent Cassini's average position simultaneous with every subexposure interval.

Furthermore, multiple flashing events in a row, i.e., in consecutive HST orbits, were observed on 6 occasions, and we found these consecutive events occur at similar spatial locations (both local time and latitude): see 2013-111, 2013-140, 2014-145, 2016-181, 2017-238 and 239 in Table 1, except for one obvious counterexample in 2016-232 when the flash location shifted against the direction of corotation from near midnight towards the afternoon sector between two observations separated by ∼1 h 45 min. Cassini's sampling of the magnetic field perturbations is dependent on its radial distance to Saturn, the latitudinal location and longitudinal location. So, we examined the most representative recurrent event (2016-232) in which Cassini was conjugate to the flashing region. Furthermore, the rare opportunities of exposures in consecutive HST orbits enabled us to find these recurrent (quasiperiodic) flashes with a variable periodicity between 60 and 90 min, although the uncertainty can be several minutes due to the time length of each subexposure. It is likely that the other flashes were also quasi-periodic but this cannot be confirmed with the limited imagery available. The images from 2013 had integration times of ∼2 min each whereas the 3 other years had longer integrations, on average ∼8 min. The flash duration was calculated based on image time tags to show in how many image frames every flash was present. Hence the periodicity and lifetime can differ in either direction, that is, the duration calculated for every flash is of order of the picture's exposure time. We found the lifetimes of these transient features to be ∼5–13 ± 2 min for 2013 and ∼5–17 ± 8 min for the 3 other years.

3.2. Cassini Magnetometer Measurements of Quasiperiodic Perturbations

We examined *in-situ* magnetic field data measured by Cassini's magnetometer with internal field subtracted for the time list of HST observations of transient auroral flashes (Table 1). On 2014-145 Cassini was located >45 Rs (see Table 1) in the dayside, i.e., outside the magnetosphere. Out of the remaining events, quasiperiodic pulsations in the MAG data were observed on ten of these days (24 h interval of observation) and simultaneous with a transient auroral flash on 6 events (2013-110, 2013-138, 2013-139, 2014-100, 2016-181 and 2016-232). The 24-h magnetic field measurements for 2013-110, 2013-138 and 2013-139 are displayed in Figure 2 corresponding to the three flashing events shown in Figure 1.

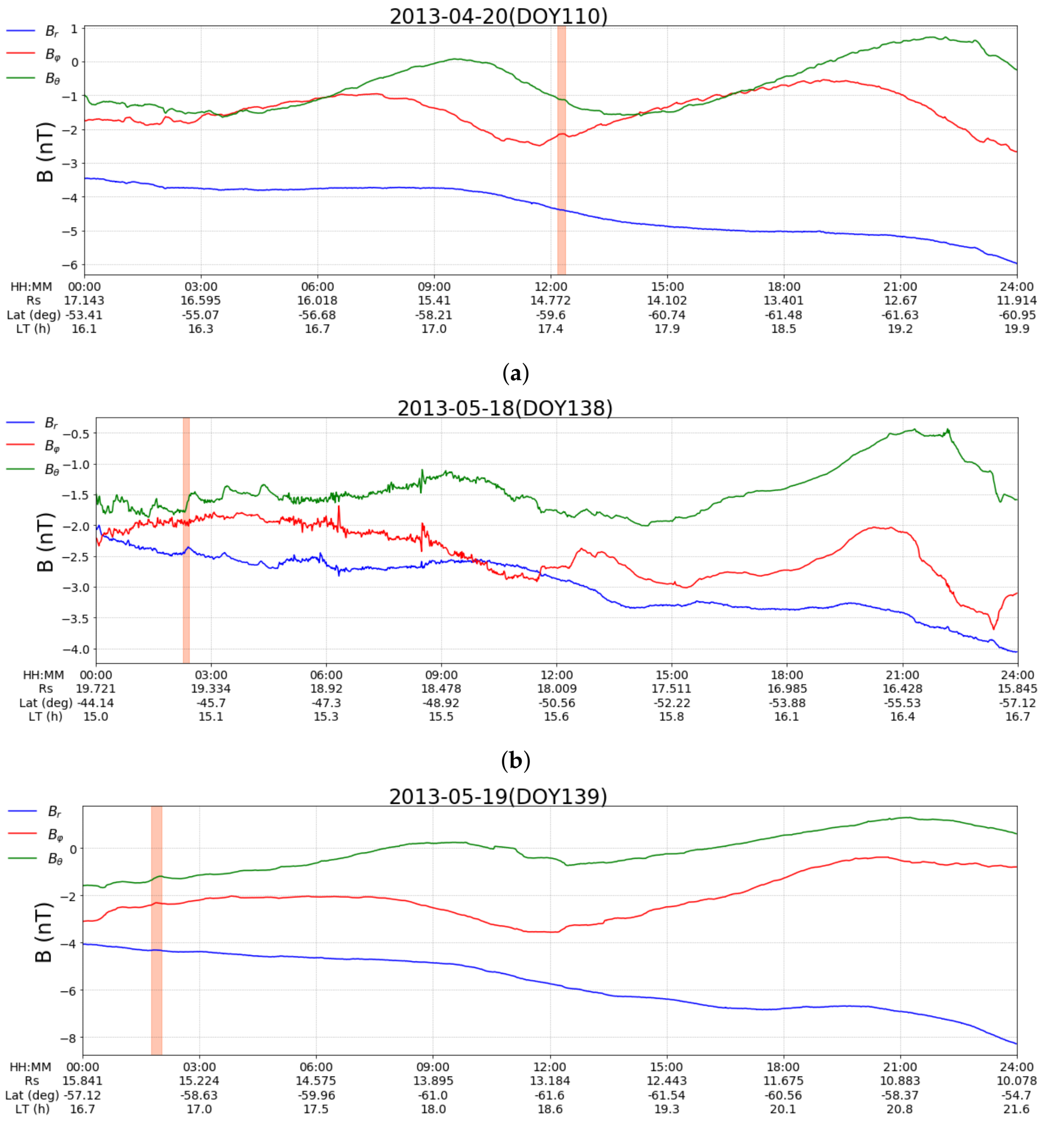

(**a**)

(**b**)

(**c**)

Figure 2. Magnetic field measurements in KRTP coordinates recorded by Cassini's magnetometer. Orange shades represent the time when a transient flash was observed by the HST. (**a**): 2013-110; (**b**): 2013-138; (**c**): 2013-139.

Table 1. List of transient flashes identified from HST images of Saturn's northern hemisphere. The data sets are illustrated with flash sequence number, "Flash start time" representing the HST-to-Saturn subexposure in which each flash is first observed, T_D the time duration (in minutes) in which the flashes were identifiable on the images, the spatial locations where flashes were switched on with respect to Local Time (in hour) and Colatitude (in degrees), the maximum intensity of each flashing episode measured in kiloRayleigh, and the average Cassini's range (in saturnian radii) away from the planet during the flash interval.

No.	Flash Start Time	T_D (m)	LT (h)	Colat (°)	I_{max} (kR)	Range (Rs)
1	2013-110 12:11:25	11.0	18–21	15	27.8	14.9
2	2013-111 12:00:02	11.0	16–20	15	37.8	9.0
3	2013-111 13:31:04	4.7	16–20	15	28.7	8.5
4	2013-113 07:04:05	6.3	18	10	35.8	12.5
5	2013-138 02:16:43	6.3	14–17	10–15	86.0	19.4
6	2013-139 01:46:36	11.0	14–18	10	45.3	15.5
7	2013-140 18:00:53	8.7	13–17	10	41.0	6.3
8	2013-140 19:08:00	9.0	13–16	10	41.2	6.2
9	2013-140 20:39:02	8.7	15–19	5–15	52.2	6.3
10	2013-141 16:04:12	13.3	14–18	10–15	33.3	10.5
11	2013-142 01:21:47	6.3	12–14	10	37.3	12.9
12	2014-097 07:55:23	11.7	13–15	15	63.3	21.0
13	2014-100 02:29:09	14.0	13–21	10–15	96.1	12.9
14	2014-102 23:42:51	7.0	18	10	49.3	26.0
15	2014-145 04:39:03	16.3	15–19	10	36.9	45.2
16	2014-145 06:24:00	14.0	17–21	5–10	64.3	45.4
17	2014-145 07:29:31	11.7	13–18	5–10	61.2	45.5
18	2016-181 03:53:59	7.5	13–16	15	66.5	10.7
19	2016-181 04:59:25	7.5	14–16	15	63.2	10.7
20	2016-181 07:04:50	5.0	15–18	10–15	72.5	10.7
21	2016-232 19:36:50	7.5	20–23	10–15	86.1	8.0
22	2016-232 21:27:15	15.0	14–20	10–15	151.2	8.2
23	2017-066 15:44:06	16.7	13–15	5–10	70.1	3.3
24	2017-088 02:29:43	8.3	15–19	15	82.0	4.0
25	2017-095 06:49:16	8.3	18	10	65.4	4.5
26	2017-154 21:04:14	8.3	15–18	5	48.8	5.0
27	2017-206 18:00:08	8.3	15	15	42.9	1.5
28	2017-238 23:45:06	8.3	18	10	54.1	3.0
29	2017-239 04:15:01	16.7	15–17	15	59.8	3.0

On 2013-110 (Figure 2a), sawtooth-shaped perturbations with small magnitudes (∼0.2 nT) are visible in the B_ϕ component throughout the whole 24-h interval shown, and several peaks in the B_θ component in the early hours can also be seen. The signals are easiest to observe in B_ϕ due to the smaller magnitude of the background field in this component. Cassini was at a radial distance of ∼15 Rs in the southern hemisphere around the time the HST images were taken (red shading). The periodicity of perturbations generally appears to be ∼1 h except that it obviously shortens to ∼20 min between 15–19 UT as previously described by Badman et al. [26]. On 2013-138 (Figure 2b) a series of at least 5 consecutive B_θ perturbations of ≤0.5 nT intensity are seen including one during the flash exposure time. This suggests that the magnetic field perturbations were of an atypical configuration, with B_θ more significant than B_ϕ which was continuously noisy for half of the day. The variability of the field suggests this was a region of hot plasma e.g., the outer magnetosphere. 2013-139 (Figure 2c) shows a quasiperiodically perturbed field in both B_ϕ and B_θ, similar to 2013-110 (Figure 2a), with Cassini located at a similar range (∼15 Rs) in the south during the flash. The perturbations are also of small magnitudes with a peak shape but occur less frequently than 2013-110 (Figure 2a). This makes the perturbations clearly distinguishable in both components only at early, middle and late hours of the day.

3.3. Case Studies: 2014-04-10 (DOY100) and 2016-08-19 (DOY232)

The first case study aims to extend the time interval in search of the dependence between multiple pulsation events and Cassini's coverage while taking the orbital bias into account. We used SPICE to obtain Cassini's trajectory from 2014-80 to 2014-120 (Figure 3a) shown as the orange path which completes an oval coverage at high latitudes. Four sequences of QP pulsation events, in total, are observed in the magnetometer data whose time duration are marked with thick red chunks. The four pulsation sequences are identified between ∼15–23 LT (duskside) at 10–15° colatitude from 2014-99 to 2014-100. Non-detection outside the duskside could be due to the higher radial distances when the spacecraft travels to the dayside.

In this case, the flash was highly dynamic and Cassini was only above the flashing region after the flash itself rotated rapidly in the direction of corotation within its 14-min lifetime (the duration of two subexposures shown in Figure 3b,c). Figure 3d,e are the MAG plots for day 2014-99 and 2014-100 with pulsations highlighted in coloured shades matching the red sections on Cassini's coverage during that period in Figure 3a. The pulsations take sawtooth shapes, variable intensity of ∼0.5–2 nT in B_ϕ and inconstant inter-pulse period of ∼40–60 min. Peak structures that correspond to the QP pulsations can also be seen in the B_θ components when the spacecraft was gradually changing its radial range. Hence it would be worthwhile to examine the MAG data in the averaged field-aligned coordinates in aid of analysing the characteristics of QP pulsations particularly when the field is in an abnormal shape. In Figure 3e, the red and blue stripes represent the two HST image frames (Figure 1b,c respectively).

In more details about the 2014-100 flash and its MAG data, the B_ϕ pulsation was detected in the blue stripe (whose start and stop time are the same as Figure 1c) with a peak followed by a very sharp drop, whereas the signal remained rather constant in the red shading. The decrease in B_ϕ indicates a transition to a less lagging field configuration as the spacecraft was at the southern hemisphere (negative B_r), this indicates that the MAG could not be measuring the pulsating field lines unless the spacecraft changed its leading position (Figure 1b) to a slightly lagging position (Figure 1c) relative to the leading end of the flash morphology. The fact that MAG did not detect a pulsation during the time of the first frame whilst it did during the second frame further proves the direct connection between transient flashes and QP pulsation events picked up in magnetic field measurements.

The duration of each event ranges from 3 to over 10 h and is separated by a gap of 2–10 h. The gaps between the sets of events could be related to the rocking of the affected field region over and away from the spacecraft, driven by the Planetary Period Oscillation (PPO) [27]. This rocking has been observed in the auroral currents and the cusp at Saturn [28,29]. However, the duration of the gaps is irregular (2–10 h), and there are other examples where gaps are not present, e.g., 2013-100 (Figure 2a). This effect could be further examined by comparing the position of the spacecraft relative to the PPO oscillation in more detail to possibly determine the boundaries of the pulsating region.

Figure 4a–c shows two separate events on 2016-232 (no.21 and no.22 in Table 1) with the MAG data displayed in Figure 4d. The yellow arrow indicates the identified transient flash and a persisting feature in the noon-dusk sector is indicated by a blue arrow. Two flashing events are observed on this day. Figure 4a shows a bright feature in the 21-0 LT sector with lifetime equal to the image integration time (450 s). This event was the only sequence being observed at a very late LT in the duskside. The distribution of location dependence of auroral flashes will be shown in the Section 3.4. Figure 4b,c show another rotating flash with twice the lifetime as the previous event (Figure 4a). This event and the 2014-100 event imply that transient flashes can rotate rapidly either following (Figure 3b,c) or countering (Figure 4b,c) the direction of corotation. In the first example, 2014-100, the flash moves from 12–18 LT (in Figure 3b) to 15–21 LT (in Figure 3c) between the two subexposures. The leading edge was moving at ∼25% of corotation rate. In the second case, 2016-232, the flash rotated from 16-20 LT (in Figure 3b) to 13–17 LT (in Figure 3c) and 5° poleward, then moved partially into the main oval at 15 LT and 10° colatitude. The edge was moving 25% of corotation speed as well but in the opposite direction of corotation contrast to the previous example (2014-100). Furthermore, both fast-rotating flashes were seen, in images with similar time integrations, when the main emission was either quiet (Figure 3b,c) or active (Figure 4a–c). This further shows that transient auroral flashes are more localised and can be independent of changes in the auroral dynamics in a global scale.

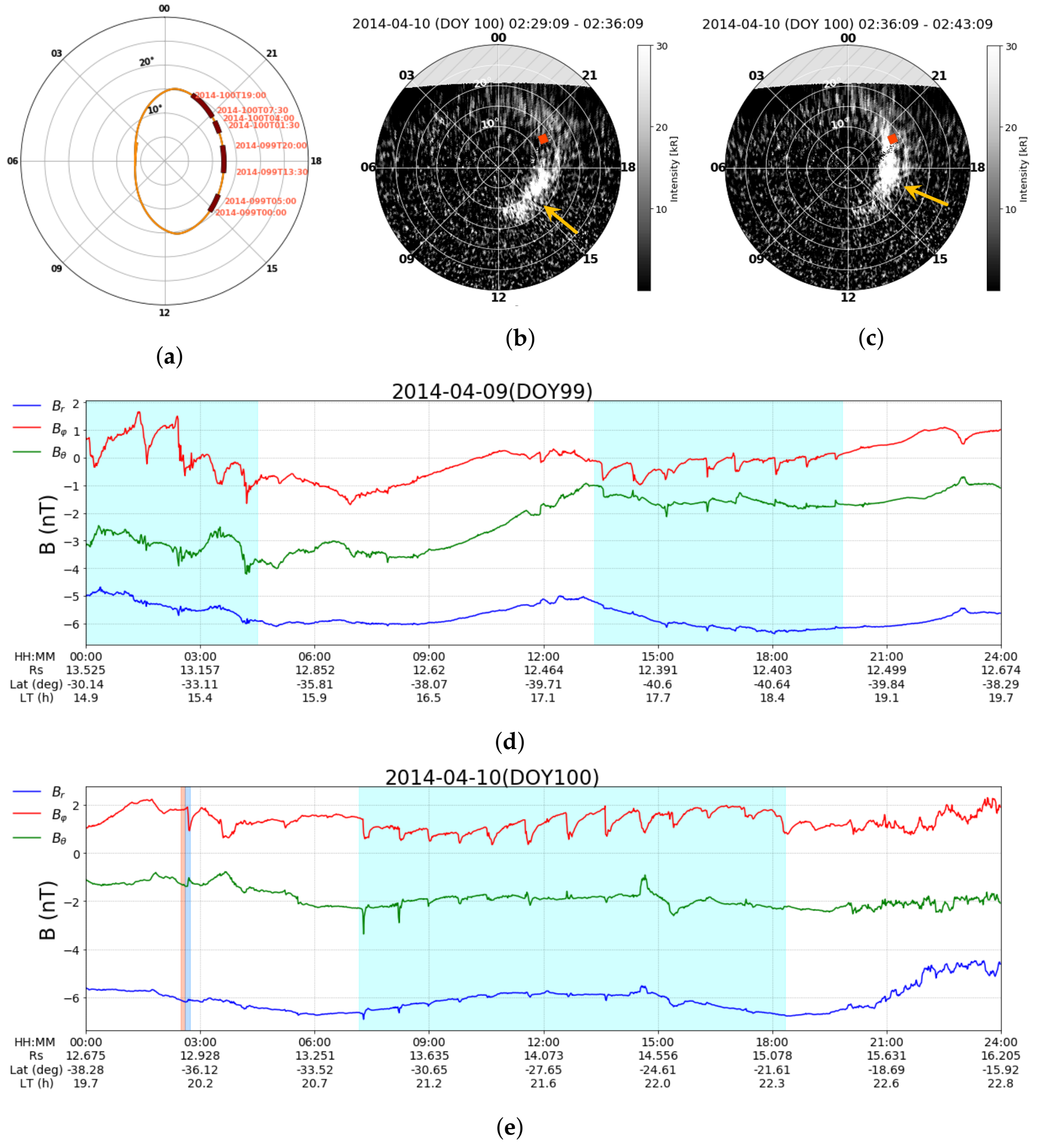

Figure 3. (**a**): Trajectory of Cassini spacecraft from 2014-80 to 2014-120 (orange path), obtained using SPICE, projected onto the Kronocentric polar plane, with 4 QP pulsation sequences identified in MAG data (red thick chunks) during this interval. (**b**,**c**): HST images of Saturn's northern hemisphere in polar projection for the frames during the 2014-100 event (sequence no.13). The polar projection is the same as Figure 1, and the integration time of the images is 420 s. (**d**,**e**): 24-h *in-situ* magnetic field measurement in KRTP coordinates by Cassini magnetometer. Red and blue stripes represent the time when a transient flash was observed by the HST, while the cyan shades highlight a series of pulsed events in the magnetic field outside of HST's observation window.

During the period of HST observations on this day, Cassini was located at ∼18 LT as indicated by the red footprint. Simultaneous with the identification of auroral flashes, two field pulsations were also recorded in the MAG data (Figure 4d) as highlighted by the orange (corresponding to the same time interval as Figure 4a) and blue (corresponding to the same time interval as Figure 4b,c) shadings. It is noticeable that during both pulsed events simultaneous with the two transient auroral flashes, the B_ϕ component exhibited a drop by ∼1 nT. The first pulsation (orange shading) indicates a less lagging field configuration as the B_ϕ diminishes, while the second represents a more leading field as the head of the auroral flash moved to earlier LT compared to Cassini's footprint.

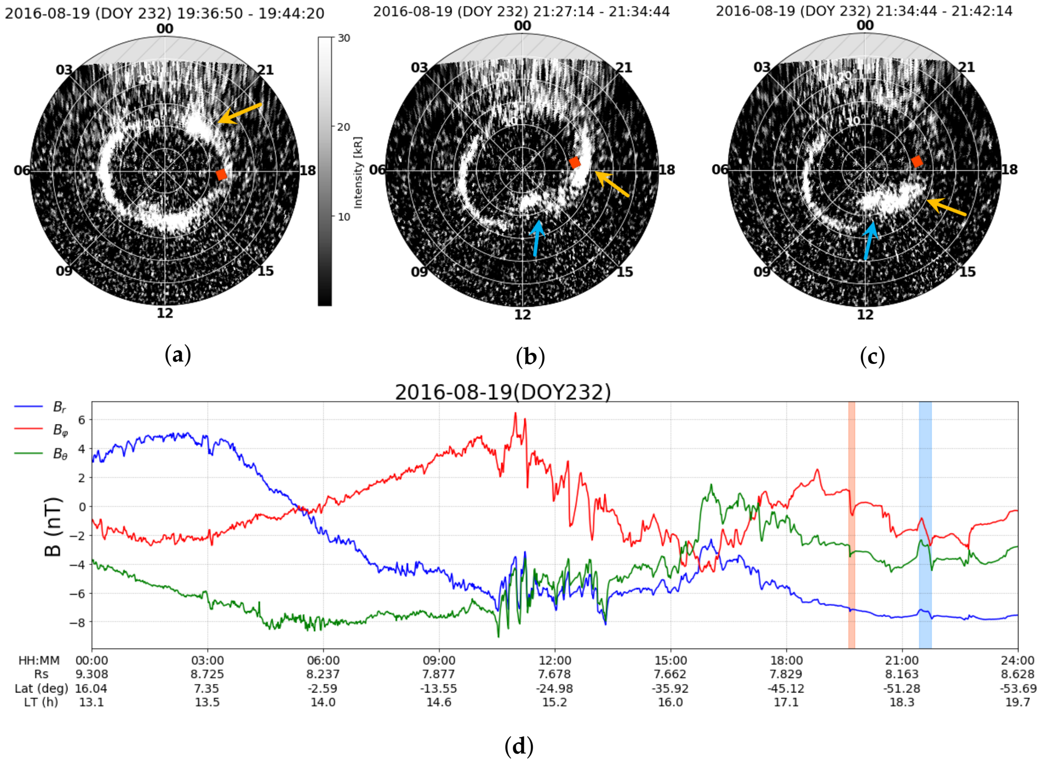

Figure 4. (**a**–**c**): HST images of Saturn's northern hemisphere in polar projection for two separate events on 2016-232, event no.21 (**a**) and event no.22 (**b**,**c**). The yellow arrows highlight the identified transient feature, and the blue arrows highlight a rather persisting feature at high latitudes in the 12-15 LT sector. The polar projection is the same as Figure 1, and the integration time of the images is 450 s. All three panels share the same colour bar as panel (**a**) represnting the auroral intensity in kiloRayleigh (kR). (**d**): 24-h *in-situ* magnetic field measurement in KRTP coordinates by Cassini magnetometer. The orange shading represents the time when the transient flashes were observed by the HST as shown in panel (**a**), and blue represents the flash shown in (**b**,**c**).

3.4. Map of Flash Distribution and Cassini Coverage

These transient auroral features may take variable shapes and non-fixed locations of occurrence as pointed out by previous studies [3,9,30], hence constructing a map of distribution ("heat map") representing their overall latitude and local time dependence would enable us to find links to particular energetic events observed in *in-situ* measurements.

The duration of flashes are generally longer than the image integration times, so an averaged pseudo-image was hence created by adding the image frames containing well distinguished transient features and averaged by the number of frames N:

$$< I >= \sum_N I/N. \tag{1}$$

This is named a pseudo-image because it does not show what was captured by the camera but an averaged distribution of a transient flashing event across several subexposures. More importantly, due to the fast rotation of Saturn, it is likely that these auroral features may change position even within a matter of minutes, the pseudo-image obtained in this step depicts the full evolution of a flash. However, the peak intensities will be lowered after averaging for those dynamic flashes.

It is also important to consider that the flash region has background brightness or may already show other types of features (e.g., the main oval or the inner arcs), we hence need to subtract the "background":

$$I_{flash} =< I > -I_{background}. \tag{2}$$

These "background" intensities are persisting and not changing dramatically over each HST exposure, so chronologically the subexposure before the flashing frame is used as the "background" frame. But this, of course, does not take into account the rotating background across several subexposures (of order several tens of minutes).

To construct a heat map for every flashing event, the sector containing the flash morphology was extracted by setting all pixels outside this sector to zero as we only want to map the transient features. A threshold intensity is chosen explicitly for every event in order to further subtract the background pixel values:

$$I_{heat} = I_{flash} - I_{threshold}. \tag{3}$$

In this case the threshold intensity was determined by the lowest intensity value within the flash region. Although the threshold intensity can sometimes be smaller than a minority of those bright background features which survived the previous background subtraction process, it is a trade off for maintaining the complete flash morphology. The non-zero pixels in our intensity array, I_{heat}, were then assigned the same value and plotted onto our heat map as we focus on the location of occurrence here instead of the actual intensity value.

A summary of Cassini's real-time footprint in all flash sequences in this study (Table 1) was made as Figure 5, and the overall coverage from different years and whether QP pulsations were seen in MAG data in each HST exposure are distinguished by different colours and shapes as labelled in the lower right corner. Cassini moved to the F-ring and proximal orbits, periapsis $\leq$ 10 Rs, in 2017 (the Grand Finale), so it's noticeable that the trajectories (in yellow) are much longer than other years within the same exposure durations. Moreover, the footprints from 2017 did not extend to 12–18 LT sector and were generally lower in latitudes, while that from other years were more towards the planet's poles—within 15° colatitude—in the noon-dusk sector where QP pulsations were mostly found. The crosses in the 15–21 LT sector are footprints in 2013-110, 138, and 139 (green), 2014-100 (red), 2016-181 and 232 (blue). The MAG data of these events were presented in Figures 2–4 respectively. We find the spatial location of the spacecraft an important factor in order to detect quasiperiodic magnetic field perturbations, and this preferential spatial location of Cassini's footprint is within 15–21 LT and 5–15° colatitude, which agrees with our observed morphological distribution of transient auroral flashes (as told from the heat map distribution in Figure 5). The first auroral flash in 2016-232 (Figure 4a) mentioned earlier was observed in the 21–0 LT sector, which is outside the preferential LT. At the same time, flashes were also observed near noon ($\sim$12 LT) but in lower populations, indicating that these transient events may occur across the entire duskside although the chances are smaller at both ends. Apart from the footprints where magnetic field perturbations were recorded by magnetometer (the coloured crosses in Figure 5), no such pulsed events were observed at lower latitudes in the preferential local-time sectors (15–21 LT), nor in the dawnside at the preferred co-latitude range (5–15°). However, it is worth noting that Cassini's *in-situ* measurements have an orbital bias as it did not cover the high latitudes in the dayside as often as it did in the duskside. Besides, Cassini's distance from the planet may also affect the detection of magnetic field signatures as the background field magnitude and direction change with distance from the planet, and the amplitude of the perturbations may also vary with distance from the planet. Nonetheless, this result indicates that QP auroral flashes and field pulsations are likely to be localised rather than being driven globally because of lack of detection in other LT and latitude regions. The spacecraft's range, location in LT and latitude combined is the key to detection of pulsations. Cassini's range for every flash sequence is listed in Table 1, we found the ranges to be 8–19.4 Rs for our detected cases which are all when Cassini was in the southern hemisphere.

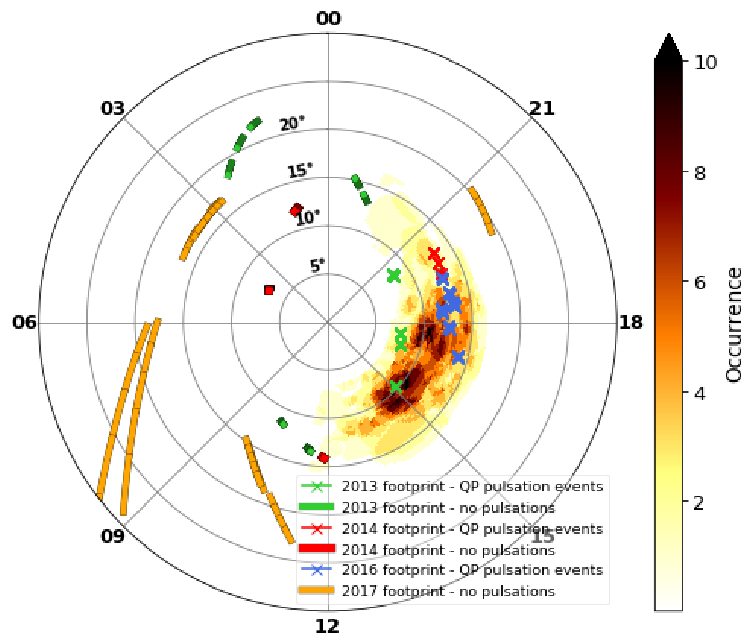

Figure 5. Summary footprint of Cassini orbiter in flash sequences identified in HST images from 2013–2017 plotted on top of "heat map" of transient flashing events. The polar projection extracts latitude from 90 to 60° (i.e., 0 to 30° colatitude) with a step of 5°. The colour scale of the "heat map" encodes the number of occurrences from plain white to dark orange with the highest value 10. The year every colour stands for is listed in lower right corner, with crosses representing the detected QP pulsations (green: 2013-110, 2013-138, 2013-139, red: 2014-100, blue: 2016-181, 2016-232).

4. Discussion and Conclusion

In this study, we examined 36 days of HST observations of Saturn's northern UV aurora during 2013–2017 and identified 29 flashes. These transient features appear for ∼4–17 min in HST subexposures, though can be subject to uncertainties related to the image integration times, and are predominantly located at ∼8–15° colatitude in the duskside (14–19 LT). In this research, more than one flashing event in the same day was found on 6 occasions (2013-111, 2013-140, 2014-145, 2016-181, 2016-232, and 2017-238 to 239) as told from Table 1 indicating these transient flashes can be recurrent leading to the quasi-periodic characteristics. The spatial distribution is in general agreement with the duskside preference from previous studies [6–9]. However, the modified Alfvén wave model developed by Rusaitis et al. [16] concluded no strong dependence of spatial location for QP pulsed events after normalising for the spacecraft's dwell time. Additionally, studies of near-noon auroral events Yao et al. [14] may imply an extended distribution to the dawnside, close to the one summarised by [9] using Cassini UVIS data.

We analysed the Cassini MAG data for the time list of HST observation of transient auroral flashes (Table 1) and identified 10 sets of QP pulsed events (6 of them occured exactly simultaneous with the HST flash exposure). The field perturbations take asymmetric sawtooth shapes with typical magnitudes ranging from ∼0.2 nT (e.g., Figure 2a,c) to 2 nT (e.g., Figure 4d) when Cassini travelled close to Saturn, and these perturbations are primarily seen in the B_ϕ component although they can less occasionally become more significant in B_θ (e.g., Figure 2b) due to different field orientation. We find Cassini's range to be 8–19.4 Rs for our detected cases (all in the southern hemisphere), this agrees with Palmaerts et al. [7] who found the dependence in range to be 5–30 Rs in the northern hemisphere and 5–20 Rs in the southern hemisphere. Hence the factors affecting the sampling of pulsation events are the combination of Cassini's spatial location in LT, latitude, and distance. Further analysis of particle data for the event list identified in this study would be an interesting extension to this study.

The pulsation events can vary from a couple of pulses to recurrent events with duration over a half day. A typical periodicity of $\sim$1 h can be found on both HST images and MAG data, which is consistent with particle and wave measurements found in other studies [3,5–9,31]. The inter-pulse period in the same event could vary, and we found different ranges using HST images (60–90 min) and Cassini MAG data (40–70 min), both lying inside the distribution concluded by other multi-instrument studies [6,7,9]. However, the underlying factor(s) for such a periodicity and its variability remain an open question.

There is no observed correlation between the occurrence of the transient flashes and Saturn's main emission power as they were observed with both strong and faint main emission. We infer that the QP events have been observed during a range of solar wind conditions, so they are unlikely to be driven by solar wind dominant mechanisms (e.g., magnetopause reconnection). Delamere et al. [10] proposed the reconnection drizzle that occurs primarily in the duskside, and Guo et al. [11,12] suggested that magnetodisc reconnection can occur on the dayside. This provides indications to the dynamic process which potentially powers the QP energetic events focused in this research with similar spatial location dependence. Moreover, the HST campaigns used in this study all captured Saturn's northern aurora while Cassini picked up periodic magnetic field perturbations in the southern hemisphere (indicated by negative B_r), suggesting QP events occur on closed field lines. Pulsations in MAG were only observed when Cassini's footprint was in the same LT-latitude sector (inside the magnetosphere) as the observed flashes, implying that the driving mechanism is localised. This needs to be accounted for in considering the origin of the flashes, e.g., if driven by a solar wind structure, this cannot impact all LT or propagate through the magnetosphere equally, otherwise a more global response would be expected. The aforementioned studies used a sharp drop in the B_θ component or negative B_θ as an identifier of current sheet crossings, however, for QP pulsations detected at high latitudes in our research, the B_θ component often shows an increase (i.e., becomes more southward) and the sharp drop is observed in the B_ϕ component (i.e., becomes less lagging). This field configuration is consistent with a localised magnetic dipolarisation, or reconnection front, in planetary magnetotails. Yao et al. [32] investigated into a number of cases of dipolarisation on Saturn and reported a localised process responsible for such events—transient dipolarising flux bundles (usually seen with a B_θ enhancement) which is supported by magnetic reconnection through a "drizzle-like" process suggested by Delamere et al. [10].

Some previous works suggested wave relations for these quasi-periodic pulsed events [13,14,16], while previous work by Bader et al. [9] pointed out the lack of wave-related characteristics for magnetic field pulsations identified in the MAG data, i.e., that the identified magnetic field perturbations in the B_ϕ component are of asymmetric sawtooth shapes instead of sinusoidal shapes, and the recurrence period of the pulsations is more variable than expected for wave signatures. However, studies of Earth's magnetosphere indicated that the symmetric and asymmetric field fluctuations can relate to different stages of development (linear [33] versus non-linear [34]) of the same process such as the kinetic ballooning interchange instability. At Jupiter, Yao et al. [35] suggested compressional waves are also associated with Jupiter's auroral pulsations. However, the Saturn flashes are very commonly seen, so the question remains whether they need a transient driver e.g., bursts of magnetodisc reconnection, or if they are symptomatic of an ongoing state of the magnetosphere.

Author Contributions: Conceptualization, T.Q., S.V.B. and A.B.; Data curation, T.Q.; Formal analysis, T.Q.; Funding acquisition, S.V.B.; Investigation, T.Q.; Methodology, T.Q., S.V.B. and A.B.; Project administration, S.V.B.; Resources, T.Q., S.V.B., J.K. and A.B.; Software, T.Q., J.K. and A.B.; Supervision, S.V.B.; Validation, T.Q. and J.K.; Visualization, T.Q.; Writing—original draft, T.Q.; Writing—review and editing, S.V.B., J.K. and A.B. All authors have read and agreed to the published version of the manuscript.

Funding: Sarah Badman was supported by STFC grant ST/M005534/1 and Sarah Badman and Joe Kinrade were supported by STFC grant ST/V000748/1.

Institutional Review Board Statement: Not applicable.

Informed Consent Statement: Not applicable.

Data Availability Statement: This research is based on publicly available observations acquired with the NASA/ESA Hubble Space Telescope and obtained at the Space Telescope Science Institute, which is operated by AURA for NASA (program IDs 13051, 13396, 14267, and 14811) (https://archive.stsci.edu/hst/search.php). Cassini Magnetometer data are available from the Planetary Plasma Interaction Node in the Planetary Data System archives (https://pds-ppi.igpp.ucla.edu/mission/Cassini-Huygens/CO/MAG).

Conflicts of Interest: The authors declare no conflict of interest.

References

1. Radioti, A.; Tomás, A.T.; Grodent, D.; Gérard, J.C.; Gustin, J.; Bonford, B.; Krupp, N.; Woch, J.; Menietti, J.D. Equatorward diffuse auroral emissions at Jupiter: Simultaneous HST and Galileo observations. *Geophys. Res. Lett.* **2009**, *36*, L07101. [CrossRef]
2. Badman, S.V.; Achilleos, N.; Arridge, C.S.; Baines, K.; Brown, R.; Bunce, E.; Coates, A.J.; Cowley, S.; Dougherty, M.; Fujimoto, M.; et al. Cassini observations of ion and electron beams at Saturn and their relationship to infrared auroral arcs. *J. Geophys. Res. Space Phys.* **2012**, *117*. [CrossRef]
3. Radioti, A.; Grodent, D.; Gérard, J.C.; Bonfond, B.; Gustin, J.; Pryor, W.; Jasinski, J.; Arridge, C. Auroral signatures of multiple magnetopause reconnection at Saturn. *Geophys. Res. Lett.* **2013**, *40*, 4498–4502. [CrossRef]
4. Meredith, C.; Cowley, S.; Hansen, K.; Nichols, J.; Yeoman, T. Simultaneous conjugate observations of small-scale structures in Saturn's dayside ultraviolet auroras: Implications for physical origins. *J. Geophys. Res. Space Phys.* **2013**, *118*, 2244–2266. [CrossRef]
5. Mitchell, D.; Carbary, J.; Bunce, E.; Radioti, A.; Badman, S.V.; Pryor, W.R.; Hospodarsky, G.; Kurth, W. Recurrent pulsations in Saturn's high latitude magnetosphere. *Icarus* **2016**, *263*, 94–100. [CrossRef]
6. Roussos, E.; Krupp, N.; Mitchell, D.; Paranicas, C.; Krimigis, S.; Andriopoulou, M.; Palmaerts, B.; Kurth, W.; Badman, S.; Masters, A.; et al. Quasi-periodic injections of relativistic electrons in Saturn's outer magnetosphere. *Icarus* **2016**, *263*, 101–116. [CrossRef]
7. Palmaerts, B.; Roussos, E.; Krupp, N.; Kurth, W.S.; Mitchell, D.G.; Yates, J.N. Statistical analysis and multi-instrument overview of the quasi-periodic 1-hour pulsations in Saturn's outer magnetosphere. *Icarus* **2016**, *271*, 1–18. [CrossRef]
8. Pan, D.X.; Yao, Z.H.; Guo, R.L.; Bonfond, B.; Wei, Y.; Dunn, W.; Zhang, B.Z.; Zong, Q.G.; Zhou, X.Z.; Grodent, D.; et al. A Statistical Survey of Low-Frequency Magnetic Fluctuations at Saturn. *J. Geophys. Res. Space Phys.* **2021**, *126*, e2020JA028387. [CrossRef]
9. Bader, A.; Badman, S.V.; Yao, Z.; Kinrade, J.; Pryor, W. Observations of continuous quasiperiodic auroral pulsations on Saturn in high time-resolution UV auroral imagery. *J. Geophys. Res. Space Phys.* **2019**, *124*, 2451–2465. [CrossRef]
10. Delamere, P.A.; Otto, A.; Ma, X.; Bagenal, F.; Wilson, R.J. Magnetic flux circulation in the rotationally driven giant magnetospheres. *J. Geophys. Res. Space Phys.* **2015**, *120*, 4229–4245. [CrossRef]
11. Guo, R.; Yao, Z.; Sergis, N.; Wei, Y.; Mitchell, D.; Roussos, E.; Palmaerts, B.; Dunn, W.; Radioti, A.; Ray, L.C.; et al. Reconnection Acceleration in Saturn's Dayside Magnetodisk: A Multicase Study with Cassini. *Astrophys. J. Lett.* **2018**, *868*, L23. [CrossRef]
12. Guo, R.; Yao, Z.; Wei, Y.; Ray, L.C.; Rae, I.; Arridge, C.S.; Coates, A.; Delamere, P.; Sergis, N.; Kollmann, P.; et al. Rotationally driven magnetic reconnection in Saturn's dayside. *Nat. Astron.* **2018**, *2*, 640–645. [CrossRef]
13. Yates, J.N.; Southwood, D.; Dougherty, M.; Sulaiman, A.H.; Masters, A.; Cowley, S.W.; Kivelson, M.; Chen, C.H.; Provan, G.; Mitchell, D.G.; et al. Saturn's quasiperiodic magnetohydrodynamic waves. *Geophys. Res. Lett.* **2016**, *43*, 11–102. [CrossRef]
14. Yao, Z.; Radioti, A.; Rae, I.; Liu, J.; Grodent, D.; Ray, L.; Badman, S.; Coates, A.; Gérard, J.C.; Waite, J.; et al. Mechanisms of Saturn's near-noon transient aurora: In situ evidence from Cassini measurements. *Geophys. Res. Lett.* **2017**, *44*, 11–217. [CrossRef]
15. Rusaitis, L.; Kivelson, M.; Khurana, K.K.; Strangeway, R.J.; Walker, R.J. Quasi-periodic 1-hour pulsations in Saturn's outer magnetosphere. In Proceedings of the AGU Fall Meeting Abstracts, Washington, DC, USA, 10–14 December 2018; Volume 2018, p. SM23E–3242.
16. Rusaitis, L.; Khurana, K.K.; Kivelson, M.; Walker, R.J. Quasiperiodic 1-hour Alfvén Wave Resonances in Saturn's Magnetosphere: Theory for a Realistic Plasma/Field Model. *Geophys. Res. Lett.* **2021**, *48*, e2020GL090967. [CrossRef]
17. Nichols, J.D.; Badman, S.; Bunce, E.; Clarke, J.; Cowley, S.W.H.; Hunt, G.; Provan, G. Saturn's northern auroras as observed using the Hubble Space Telescope. *Icarus* **2016**, *263*, 17–31. [CrossRef]
18. Kinrade, J.; Badman, S.V.; Provan, G.; Cowley, S.; Lamy, L.; Bader, A. Saturn's northern auroras and their modulation by rotating current systems during late northern spring in early 2014. *J. Geophys. Res. Space Phys.* **2018**, *123*, 6289–6306. [CrossRef]
19. Lamy, L.; Prangé, R.; Tao, C.; Kim, T.; Badman, S.; Zarka, P.; Cecconi, B.; Kurth, W.; Pryor, W.; Bunce, E.; et al. Saturn's northern aurorae at solstice from HST observations coordinated with Cassini's grand finale. *Geophys. Res. Lett.* **2018**, *45*, 9353–9362. [CrossRef]

20. Clarke, J.; Nichols, J.; Gérard, J.C.; Grodent, D.; Hansen, K.; Kurth, W.; Gladstone, G.; Duval, J.; Wannawichian, S.; Bunce, E.; et al. Response of Jupiter's and Saturn's auroral activity to the solar wind. *J. Geophys. Res. Space Phys.* **2009**, *114*. [CrossRef]
21. Gustin, J.; Bonfond, B.; Grodent, D.; Gérard, J.C. Conversion from HST ACS and STIS auroral counts into brightness, precipitated power, and radiated power for H2 giant planets. *J. Geophys. Res. Space Phys.* **2012**, *117*. [CrossRef]
22. Dougherty, M.; Kellock, S.; Southwood, D.; Balogh, A.; Smith, E.; Tsurutani, B.; Gerlach, B.; Glassmeier, K.H.; Gleim, F.; Russell, C.; et al. The Cassini magnetic field investigation. *Cassini-Huygens Mission.* **2004**, 331–383.
23. Dougherty, M.K.; Cao, H.; Khurana, K.K.; Hunt, G.J.; Provan, G.; Kellock, S.; Burton, M.E.; Burk, T.A.; Bunce, E.J.; Cowley, S.W.; et al. Saturn's magnetic field revealed by the Cassini Grand Finale. *Science* **2018**, *362*, eaat5434. [CrossRef]
24. Bunce, E.; Cowley, S.; Alexeev, I.; Arridge, C.; Dougherty, M.; Nichols, J.; Russell, C. Cassini observations of the variation of Saturn's ring current parameters with system size. *J. Geophys. Res. Space Phys.* **2007**, *112*. [CrossRef]
25. Sorba, A.; Achilleos, N.; Sergis, N.; Guio, P.; Arridge, C.; Dougherty, M. Local time variation in the large-scale structure of Saturn's magnetosphere. *J. Geophys. Res. Space Phys.* **2019**, *124*, 7425–7441. [CrossRef]
26. Badman, S.V.; Provan, G.; Bunce, E.J.; Mitchell, D.; Melin, H.; Cowley, S.W.H.; Radioti, A.; Kurth, W.; Pryor, W.; Nichols, J.; et al. Saturn's auroral morphology and field-aligned currents during a solar wind compression. *Icarus* **2016**, *263*, 83–93. [CrossRef]
27. Provan, G.; Cowley, S.; Lamy, L.; Bunce, E.; Hunt, G.; Zarka, P.; Dougherty, M. Planetary period oscillations in Saturn's magnetosphere: Coalescence and reversal of northern and southern periods in late northern spring. *J. Geophys. Res. Space Phys.* **2016**, *121*, 9829–9862. [CrossRef]
28. Bunce, E.J.; Grodent, D.; Jinks, S.; Andrews, D.J.; Badman, S.; Coates, A.J.; Cowley, S.; Dougherty, M.; Kurth, W.; Mitchell, D.; et al. Cassini nightside observations of the oscillatory motion of Saturn's northern auroral oval. *J. Geophys. Res. Space Phys.* **2014**, *119*, 3528–3543. [CrossRef]
29. Arridge, C.S.; Jasinski, J.; Achilleos, N.; Bogdanova, Y.; Bunce, E.; Cowley, S.W.; Fazakerley, A.; Khurana, K.; Lamy, L.; Leisner, J.; et al. Cassini observations of Saturn's southern polar cusp. *J. Geophys. Res. Space Phys.* **2016**, *121*, 3006–3030. [CrossRef]
30. Badman, S.V.; Masters, A.; Hasegawa, H.; Fujimoto, M.; Radioti, A.; Grodent, D.; Sergis, N.; Dougherty, M.; Coates, A.J. Bursty magnetic reconnection at Saturn's magnetopause. *Geophys. Res. Lett.* **2013**, *40*, 1027–1031. [CrossRef]
31. Carbary, J.; Kurth, W.; Mitchell, D. Short periodicities in low-frequency plasma waves at Saturn. *J. Geophys. Res. Space Phys.* **2016**, *121*, 6562–6572. [CrossRef]
32. Yao, Z.; Grodent, D.; Ray, L.; Rae, I.; Coates, A.; Pu, Z.; Lui, A.; Radioti, A.; Waite, J.; Jones, G.; et al. Two fundamentally different drivers of dipolarizations at Saturn. *J. Geophys. Res. Space Phys.* **2017**, *122*, 4348–4356. [CrossRef]
33. Panov, E.; Sergeev, V.; Pritchett, P.; Coroniti, F.; Nakamura, R.; Baumjohann, W.; Angelopoulos, V.; Auster, H.; McFadden, J. Observations of kinetic ballooning/interchange instability signatures in the magnetotail. *Geophys. Res. Lett.* **2012**, *39*. [CrossRef]
34. Panov, E.V.; Baumjohann,W.; Nakamura, R.; Pritchett, P.L.; Weygand, J.M.; Kubyshkina, M.V. Ionospheric footprints of detached magnetotail interchange heads. *Geophys. Res. Lett.* **2019**, *46*, 7237–7247. [CrossRef]
35. Yao, Z.; Dunn, W.R.; Woodfield, E.E.; Clark, G.; Mauk, B.H.; Ebert, R.W.; Grodent, D.; Bonfond, B.; Pan, D.; Rae, I.J.; et al. Revealing the source of Jupiter's X-ray auroral flares. *Sci. Adv.* **2021**, *7*, eabf0851. [CrossRef]